Intramolecular Vibrational Force Fields for Linear Carbon Chains through an Adaptative Linear Scaling Scheme

ARTICLE *in* THE JOURNAL OF PHYSICAL CHEMISTRY A · DECEMBER 2007

Impact Factor: 2.69 · DOI: 10.1021/jp0757006 · Source: PubMed

Intramolecular Vibrational Force Fields for Linear Carbon Chains through an Adaptative Linear Scaling Scheme

Matteo Tommasini,* Daniele Fazzi, Alberto Milani, Mirella Del Zoppo, Chiara Castiglioni, and Giuseppe Zerbi

Center for NanoEngineered MAterials and Surfaces (NEMAS), Dipartimento di Chimica, Materiali e Ingegneria Chimica, G. Natta, Politecnico di Milano, P.zza Leonardo da Vinci 32, I-20133 Milan, Italy

Received: July 20, 2007; In Final Form: August 29, 2007

In this work, the vibrational force fields of hydrogen-capped oligoynes of increasing chain lengths are investigated by means of density functional theory calculations. It is shown that the interaction force constants between CC stretching coordinates decrease slowly with the distance between the two bonds considered. The consequence for the frequency dispersion of longitudinal optical (LO) phonons of an infinite polyyne chain is discussed and related to the observed behavior of the spectra of finite-size molecules. Effects of the exchange-correlation functional and of the basis set on the vibrational force constants are also investigated and the need for a scaling procedure is pointed out. Accordingly, new force fields which allow predictions in very good quantitative agreement with the available experimental data for oligoynes have been obtained, providing a sound assignment of α and β lines.

I. Introduction

Many experiments[1−7] and theoretical studies[8−16] indicate that linear chains of sp carbon atoms (polyynes) show interesting nonlinear optical properties and peculiar electronic transport properties. Furthermore, their presence has been recently revealed in carbon clusters and carbon nanotubes.[17−19] For these reasons, polyynes have recently attracted the interest of many researchers both from the experimental and the theoretical point of view.[14] Last but not least, polyynes are the real systems, which more closely resemble the early models of 1D atomic chains, which have been central in the development of solid-state physics.[20,21]

Raman spectroscopy is widely used for studying carbon nanostructured materials.[22] Therefore, an accurate modeling of their vibrational properties is highly desirable for a better understanding of this class of materials through vibrational spectroscopy.

Although the study of longitudinal vibrations of an ideally infinite polyyne chain is very simple from the mathematical point of view, the physics involved is not trivial due to the presence of long-range interactions associated with the delocalized nature of π electrons. This fact is ascribed to the relevant electron−phonon coupling, a common characteristic of many polyconjugated organic systems.[22] The investigation of the vibrational properties of polyynes can therefore provide useful informations on π-electron delocalization and related electronic properties. In a recent paper, we have shown that phonon dispersion curves of an infinite linear carbon chain are strictly related to the semiconductive character of this system.[23] Moreover, the behavior of the phonon dispersion near the Γ point of the first Brillouin zone (BZ) is reminiscent of the occurrence of a Kohn anomaly at $q = \pi/a$ in the limiting case of a cumulenic structure (one atom per cell, with periodicity a). This effect is modulated by the degree of π-electron confinement, responsible for the characteristic "dimerized" (Peierls-distorted) equilibrium structure with the consequent doubling of the crystal unit cell and opening of the electronic energy gap between π and π^* states. The simulation of infinite chains, characterized by different degrees of bond length alternation (BLA $= R_{C-C} - R_{C\equiv C}$) has shown to give markedly different longitudinal optical (LO) phonon dispersions.[23]

In this paper, we present a detailed description of the vibrational dynamics of polyynes based on first-principles calculations. The performances of different theoretical methods in predicting the effect of π-electron delocalization on the intramolecular potential are analyzed on the basis of experimental Raman data.[3] A new scaling procedure of the theoretical force constants is proposed, and the spectroscopic assignment of the so-called α and β lines[24] is given.

II. Theoretical Methods and DFT Calculations

Simulation of the Raman spectra is usually handled in the hypothesis of mechanical and electrical harmonicity.[25−27] The harmonic intramolecular potential energy can be expressed on the basis of internal coordinates; in this case, the vibrational frequencies are obtained by solving the following eigenvalue problem[26]

$$\mathbf{GFL}_k = \omega_k^2 \mathbf{L}_k \tag{1}$$

where **F** is the force constant matrix in internal coordinates, **G** is the kinetic matrix, $\omega_k = 2\pi\nu_k$, where ν_k is the vibrational frequency of the kth normal mode, and the eigenvector $\mathbf{L}_k$ describes the normal modes of vibration.

If one assumes a perfectly linear structure for polyynes ($D_{\infty h}$ point group symmetry), it is possible to obtain an exact separation of the vibrational space into two orthogonal subspaces belonging to different symmetry species (Σ for stretching coordinates and Π for linear bending coordinates).[36] This allows restriction of the study to longitudinal vibrations; their description can be worked out on the basis of a subset of internal coordinates containing just bond stretchings (CC and CH). This is justified for several reasons.

10.1021/jp0757006 CCC: $37.00
Published on Web 10/17/2007

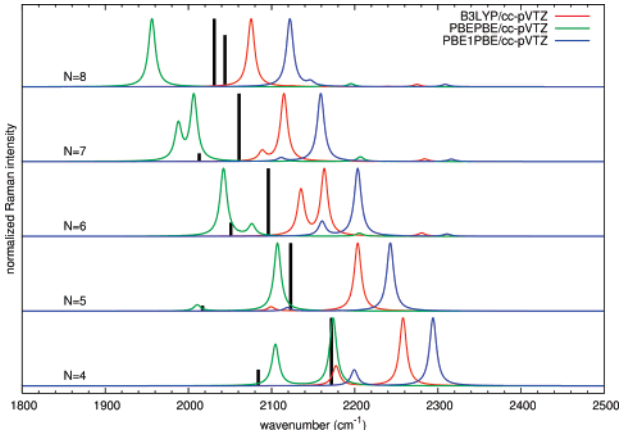

Figure 1. DFT simulations of the Raman spectrum of the polyynes H−C_{2N}−H (with $4 \leq N \leq 8$) carried out with hybrid (B3LYP, PBE1PBE) and pure (PBEPBE) functionals, compared to experimental Raman data (reported here as black vertical sticks whose heights are proportional to the relative Raman intensity).[24] All of the calculations have been carried out by using the cc-pVTZ basis set.

(a) Strongly Raman-active transitions of polyynes (spectral region between 2000 and 2200 cm^{-1}) correspond to collective CC stretchings,[2,24] that is, to longitudinal vibrations of the chain.

(b) It is known that delocalization/confinement of π electrons is relevant in affecting the terms of the intramolecular potential, which depend on CC stretching coordinates.

(c) No experimental information is available on low-frequency bending transitions, which, so far, have not been observed in the Raman or in the infrared spectra.

A. Prediction of Vibrational Frequencies. In Figure 1, the experimental Raman spectra of polyynes of increasing length are compared with the results of DFT calculations, carried out with different exchange-correlation functionals (B3LYP, PBEPBE, and PBE1PBE) and with a polarized triple split basis set (cc-pVTZ) using the Gaussian03[28] package.

Several observations can be made. (i) The experimental spectrum of all the molecules shows two well-defined Raman lines. The strongest one (α line) undergoes a continuous frequency softening with N (N = number of triple bonds in the chain); the weaker line (β line) does not follow a simple trend. Moreover, its intensity behavior (relative to the main line) shows a non-monotonic evolution. (ii) Although the numerical agreement between predicted and experimental Raman frequencies is not good (discrepancies of the order of 100 cm^{-1} are found), the observed frequency softening of the main line is predicted by all DFT calculations considered here. However, a closer look at the predicted trends indicates that DFT theory always gives a steeper dispersion than experimental spectra. (iii) As experimentally observed, calculations indicate that a second, minor feature appears in the Raman spectra. This line is assigned to the observed β peak.[24] Both the calculated frequencies and relative intensities of this line are not in good agreement with experiments. Sometimes (see $N = 6$ calculation), the predicted frequency ordering of the α and β lines is opposite to the experimental one.

Observations (i)−(iii) suggest that a satisfactory numerical agreement between calculations and experiments can be obtained only by application of a suitable scaling procedure of the DFT-computed force fields. The same conclusion was stated in ref 29, where a force-field scaling was proposed and applied with rather good success. The new scaling procedure developed in this work and the results obtained will be discussed in detail in section III.

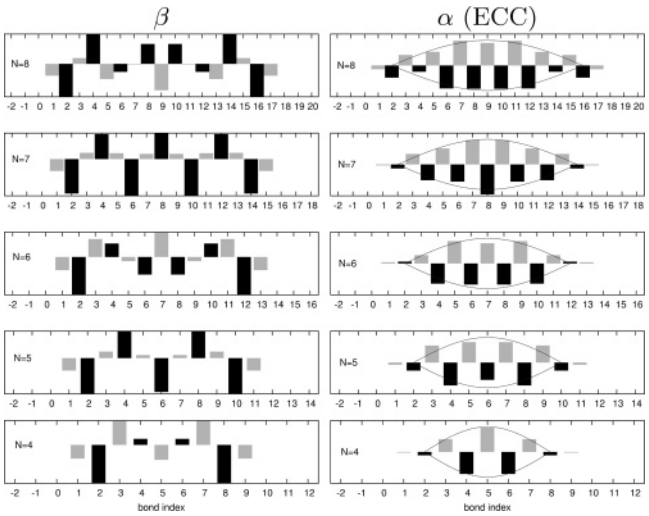

Figure 2. Eigenvectors relative to β and α lines of Raman spectra obtained from unscaled PBE1PBE/cc-pVTZ calculations for the oligoynes series with $4 \leq N \leq 8$. Gray bars represent the bond length changes associated with single bonds, while the black bars are relative to triple bonds.

So far, based on the *qualitative* agreement between calculations and experimental trends, we propose a deeper analysis of the results. This analysis will provide indications on how to build a reasonable scaling procedure. The following discussion will be devoted to (a) the vibrational assignment of both α and β lines, in particular, the vibrational assignment of the β line, which has not yet been given so far, and (b) the rationalization of the mechanism which leads to the softening of the α line and the explanation of the different behavior of the β line.

In Figure 2, the eigenvectors obtained from calculations for oligoynes ranging from $N = 4$ to 8 are sketched. It can be immediately realized that for all of the chain lengths, the eigenvector associated to the α line describes a collective out-of-phase stretching of the triple bonds (black bars) with respect to the single bonds (gray bars). This vibration is closely related to the LO phonon of the infinite polyyne chain at the Γ point ($q = 0$), which can be described as the "oscillation" of BLA. In oligoynes, this normal mode is thus the counterpart of the so-called effective conjugation coordinate (ECC coordinate), already introduced in the study of the vibrational dynamics of polyenes and polyacetylene.[22] Moreover, it is worth recalling that the BLA oscillation of an infinite polyyne exactly coincides with the $q = 0$ LO phonon; in polyacetylene, it is just a vibrational coordinate. In this case, the two strongly Raman-active phonons are due to BLA oscillation coupled with CH wagging vibrations.[22] By joining the bars in Figure 2 along the chain, a line showing the characteristic shape of a "quasi-phonon" confined into a finite size domain is obtained. The vibrational displacements lie on a stationary wave with nodes located at the end of the molecule.

The eigenvectors of the β line show the following characteristics (see Figure 2): (1) All triple bonds stretch, while the contribution of the single-bond stretching is generally negligible. This is evident especially in the case of the chains with an odd number of triple bonds. (2) In the case of chains with an odd number of triple bonds ($N = 5, 7$), the triple bonds of adjacent units oscillate out-of-phase. The wave which describes the profile of the normal mode shows, respectively, 4 and 6 nodes along the chain, that is, $N - 1$ nodes. These normal modes can be made to correspond to a phonon of the dimerized infinite chain, that is, to the phonon located on the LO branch at the BZ edge ($q = \pi/c$), which is exactly described as a pure out-

of-phase stretching of the stiffer (triple) bonds. (3) For chains with an even number of triple bonds ($N = 4, 6, 8$), the inversion center is located on the central single bond, and the shape of the eigenvector is more complex. Considering one-half of the chain, it is found that adjacent triple bonds stretch with opposite signs. However, according to the "gerade" character of the mode, the triple bonds related by inversion symmetry must exhibit the same displacement (same sign). Consistently, the two inner triple bonds show identical displacements, a fact which results in an eigenvector showing $N - 2$ nodes along the chain (one node less than the previous case).

From (2) and (3) above, we can conclude that the Raman-active normal modes associated to the β line have a different character for even and odd chains; this implies that their frequency trends should be discussed by taking into account such an even/odd effect (see also section III of Supporting Information). Indeed, a closer look at the experimental data shows that β lines of even chains practically do not exhibit frequency dispersion with chain length, while the β lines of odd chains undergo a clear frequency softening as the size of the chain increases.

B. Comparison with Phonons of the Infinite Model. The clear relation between α modes and the $q = 0$ LO phonon of the 1D crystal, as well as the correspondence between the β modes of odd chains and the $q = \pi/c$ LO phonon, suggests a discussion of our results by exploiting the simple mathematics, which describe the longitudinal phonons of an infinite "dimerized chain". This problem can be analytically worked out in terms of the force constants collected in the **F** matrix (see Supporting Information). In particular, for the optical phonons at $q = 0$ and at π/c, one obtains the following expressions[23]

$$q = 0 \quad \omega^2 = \frac{4F_{\mathscr{R}}}{m}$$

$$F_{\mathscr{R}} = \frac{k_1 + k_2}{2} + \sum_{n \geq 1} [f^n_1 + f^n_2 - 2f^n_{12}] \qquad (2)$$

$$q = \frac{\pi}{c} \quad \omega^2 = \frac{2F_{\pi}}{m}$$

$$F_{\pi} = k_1 + \sum_{n \geq 1} 2(-1)^n f^n_1 \qquad (3)$$

where m is the mass of carbon and $F_{\mathscr{R}}$ and F_{π} are the collective force constants whose explicit expressions in terms of stretching interactions are given. The k_1 and k_2 are the diagonal stretching force constants relative to the two bonds r_1 and r_2; the terms f^n describe interaction stretching force constants at increasing distances (n) along the chain.[37] When interaction force constants f are negligible, eqs 2 and 3 reduce to the well-known results of the classical textbook problem[21] of the diatomic linear chain of identical atoms connected by springs of alternating strengths (dashed line in the dispersion curves of Figure 3). However, calculations on polyynes show that interaction force constants are far from negligible. They follow the general rules which hold for any sequence of CC bonds with conjugated π electrons (e.g., polyenes[22]). These rules include the following. (i) The interaction force constants between equivalent bonds (f^n_i) are always negative; (ii) interactions between nonequivalent (single/triple) bonds (f^n_{12}) are positive; and (iii) the absolute values of the constants f^n slowly decrease with increasing n; due to conjugation, long-range interactions take place.

These rules can be verified by inspecting the **F** matrix reported in the Supporting Information. As a consequence, the sum in eq 2 contains a large number of nonvanishing terms which sum up to a relatively large negative value, therefore providing a contribution which lowers the force constant $F_{\mathscr{R}}$ and hence softens the vibrational frequency. According to eq 2, the frequency lowers either for the increase of the absolute values of the parameters f^n or for the increase of the extent of the effective interaction (number of terms in the sum). This softening of the LO phonon at $q = 0$ is illustrated in Figure 3, where the dispersion branches (full lines) have been obtained by introducing long-range interaction force constants transferred from the oligoyne with $N = 7$ into the **F** matrix of the 1D crystal.[38]

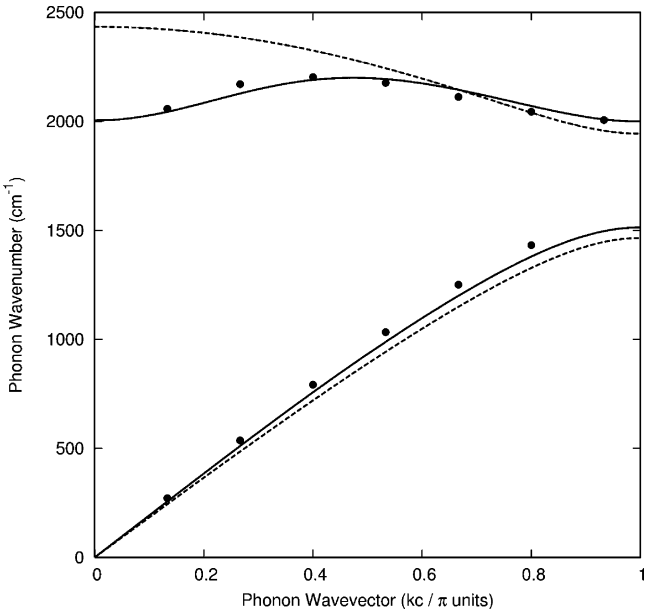

Figure 3. LO and LA phonon dispersion curves (full lines) calculated by using the scaled force field of the molecule with $N = 7$ triple bonds (PBE1PBE/cc-pVTZ). Vibrational frequencies for this oligomer are reported (black dots) as indicated in the Supporting Information (see eq 3 and related discussion). For comparison, the phonon curves obtained by removing all long interactions (f^n terms in eqs 2 and 3) are reported as dashed lines. These curves are identical to the analytical functions obtained by solving the classical textbook problem for a one-dimensional diatomic chain.[21]

Kinetic factors (the effective mass of the $q = \pi/c$ phonon is doubled with respect to that of the $q = 0$ phonon; see eqs 2 and 3) imply that the LO frequency at the zone edge has a lower frequency with respect to that at $q = 0$ (dashed lines in Figure 3). On the contrary, when long-range dynamic interactions are taken into account we obtain an anomalously low frequency at the Γ point, while the frequency at $q = \pi/c$ is weakly effected, as it can be rationalized with the help of eq 3. Since the negative interaction force constants between triple bond stretching enter the sum defining F_{π} with alternate signs, a partial cancellation of the contributions of long-range interactions occurs.

The force constants used in the calculation of the dispersion relations of Figure 3 were transferred from the scaled force field of the polyyne with $N = 7$; however, the same *qualitative* behavior would have been found using numerical parameters derived from any other polyyne at any level of theory. Nevertheless, the *quantitative* results would have been different according to the different extent of conjugation (different range of interaction and different decay law of stretching interactions). In particular, force fields transferred from longer oligomers give a more-pronounced softening of the $q = 0$ optical mode, consistent with ref 23.

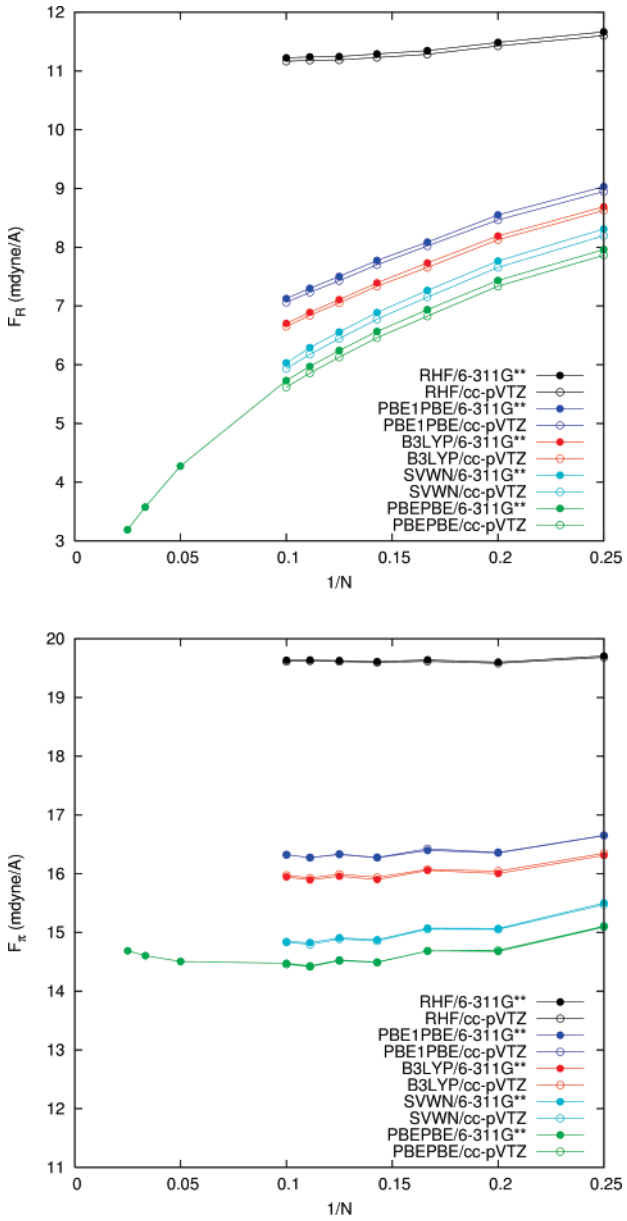

Figure 4. Values of $F_{\mathscr{R}}$ and F_π calculated with eqs 2 and 3, respectively, versus the inverse of the number of triple bonds of oligoynes. The data reported here have been obtained with hybrid DFT functionals (B3LYP, PBE1PBE) and pure DFT functionals [SVWN (LDA) and PBEPBE (GGA)]. Values from RHF calculations are plotted for a comparison. The basis sets adopted (cc-pVTZ and 6-311G**) have a minimal effect on $F_{\mathscr{R}}$ and F_π.

As shown in Figure 4, the above observations can be summarized by examining the values of $F_{\mathscr{R}}$ and F_π computed according to eqs 2 and 3, making use of the force constants obtained from different first-principles calculations on hydrogen-capped oligoynes of increasing length. Notice that in eqs 2 and 3, the diagonal force constants k_1 and k_2 of the central unit (single and triple bond) of each chain and the off-diagonal force constants relative to this unit have been used. In this way, we take into account the confinement effects due to the finite length of the molecule. As expected, the increase of π-electron delocalization with chain length results in an evident decrease of the value of $F_{\mathscr{R}}$ and in a softening of the corresponding $q = 0$ phonon. The close correlation between this phonon and the α mode of the finite-size chains rationalizes the observed frequency dispersion with increasing size.

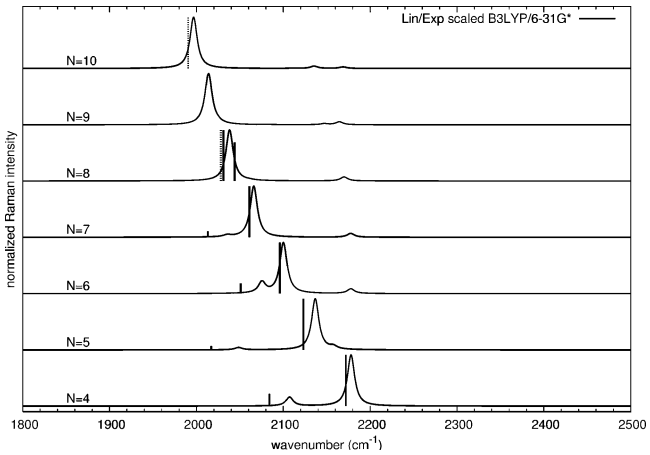

Figure 5. Simulation of the dispersion of the Raman spectra of polyynes of increasing lengths according to the Lin/Exp scaling[29] of B3LYP/6-31G* first-principles calculations. Solid vertical sticks represent the position and the relative Raman intensities of α and β lines of hydrogen-capped oligoynes.[24] Dashed vertical sticks represent the position of the α line (the only one experimentally observed) of adamantyl-capped oligoynes with $N = 8$ and 10 triple bonds.[34]

The data reported in Figure 4 show a strong dependency of the trend of $F_{\mathscr{R}}$ with the kind of theoretical approach adopted, a fact that is, in turn, related to the different frequency dispersions obtained in the simulation of the Raman spectra of oligoynes (Figure 1). This point is discussed in detail in the Supporting Information. In Figure 4, the plots for F_π are also reported. As expected, on the basis of the previous discussion of eq 3, the increase of chain length has a very small influence on the value of F_π. The minor changes that are observed are mainly due to a modest modulation of diagonal force constants with increasing chain lengths.

The suggested relationship between phonons of the 1D crystal and normal modes of oligomers can be formalized quantitatively with the help of simple mathematical models.[30] The details of how this can be done are given in the Supporting Information; the results are illustrated in Figure 3.

III. Scaling DFT Calculations

Several scaling factors have been applied to first-principles vibrational frequencies in order to obtain a better agreement with the experimental data.[31] In our case, a mere multiplicative scaling of the frequencies cannot account for the true dispersion of the α line with molecular size. Therefore, one has necessarily to consider more sophisticated scaling schemes, acting directly on the vibrational force field.[32] A scaling procedure (named Lin/Exp by the authors and applied to B3LYP/6-31G* predictions) has been recently proposed for polyynes,[29] according to which an explicit scaling of long-range interactions between different CC bonds has been suitably included into Pulay's SQM scheme.[32] The performance of this procedure can be seen in Figure 5, where the scaled results from B3LYP/6-31G* are compared to recent experimental data obtained from Raman spectroscopy.[24,33] As one can immediately see, the agreement with the experimental data for the α line is satisfactory, demonstrating the physical soundness of this approach in describing the correct dispersion of the strongest Raman line. However, the Lin/Exp scaling does not perform equally well in reproducing the minor features of the spectra (β line).

With the purpose of reproducing the relative positions and intensities of both the α and β lines, we apply a linear scaling of the results from PBE1PBE/cc-pVTZ calculations,[39] introduc-

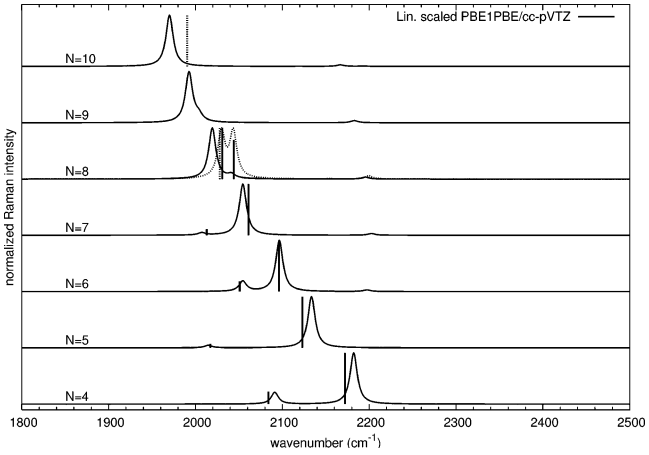

Figure 6. Raman spectra of oligoynes with $4 \leq N \leq 8$ obtained with PBE1PBE/cc-pVTZ calculations by scaling the force constant matrix according to eq 4 with $x_1 = 0.904$ and $x_2 = 0.900$. For $N = 8$, the dashed line represents the spectrum obtained by using slightly different scaling factors ($x_1 = 0.9019$ and $x_2 = 0.861$). Solid vertical sticks represent the position and the relative Raman intensities of α and β lines of hydrogen-capped oligoynes.[24] Dashed vertical sticks represent the position of the α line (the only one experimentally observed) of adamantyl-capped oligoynes with $N = 8$ and 10 triple bonds.[34]

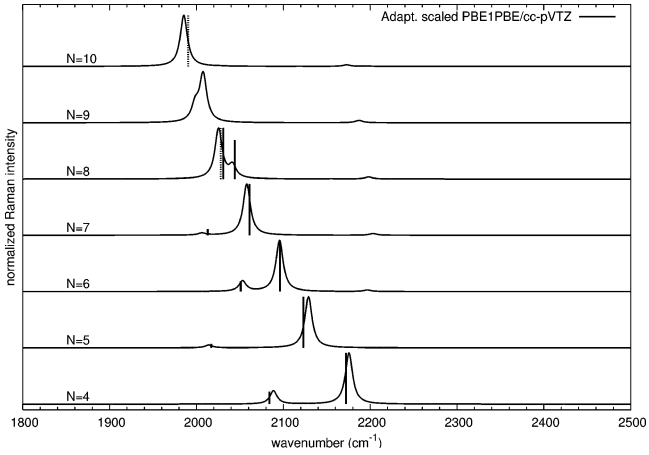

Figure 7. Raman spectra of oligoynes with $4 \leq N \leq 8$ obtained with PBE1PBE/cc-pVTZ calculations scaled with the linear adaptative procedure (see text). Solid vertical sticks represent the position and the relative Raman intensities of α and β lines of hydrogen-capped oligoynes.[24] Dashed vertical sticks represent the position of the α line (the only one experimentally observed) of adamantyl-capped oligoynes with $N = 8$ and 10 triple bonds.[34]

ing two parameters, namely, $x_1 = 0.904$ for diagonal and $x_2 = 0.900$ for off-diagonal matrix elements

$$F'_{ij} = [x_1\delta_{ij} + x_2(1 - \delta_{ij})]F_{ij} \tag{4}$$

where F'_{ij} are the matrix elements of the scaled force field. For the sake of simplicity, we use the same x_1 and x_2 scale factors also for the CH stretchings (interestingly, satisfactory results can be obtained already without a separate scaling procedure for CH stretching interactions). The Raman intensities associated with the normal modes relative to the scaled force field have been recomputed according to standard formulations of nonresonant Raman intensity.[25−27]

The comparison of the linearly scaled PBE1PBE/cc-pVTZ simulated Raman spectra with the experimental data is shown in Figure 6. As one immediately sees, the agreement for the α and β lines is good for relative Raman intensities, but the calculated frequencies do not reproduce the correct experimental dispersion of the main line. The relative position of the two lines is therefore the result of a delicate balance between diagonal and off-diagonal force constants, as already suggested by the discussion reported in section II.B. Furthermore, the relatively poorer fit of the longest hydrogen-capped polyyne, C16 (see Figure 6), can be significantly improved by reoptimizing the scaling parameters x_1 and x_2 for this molecule alone (obtaining $x_1 = 0.9019$ and $x_2 = 0.861$). In this way, the α and β bands shift toward the experimental data, and the relative intensity ratio significantly improves.

The need for specific scaling parameters in the case of C16 and the request for a better agreement with the experimental dispersion of the α line suggests a further improvement of the linear scaling. Recalling that the dispersive behavior of the α line is essentially ruled by the off-diagonal interactions, we introduce a suitable correction for the x_2 scaling parameter. Such a correction must lower the interaction range for longer chains ($N > 6$). In other words, the x_2 coefficient has to be adapted to the different polyyne lengths ("adaptative linear scaling") and becomes a suitable function of the interaction range, estimated from the force field itself. The details of this procedure are given in Appendix A. The physical meaning of this scaling scheme can justified by recalling that, in polyconjugated systems, the force constants F_{ij} are related to *delocalized* bond−bond polarizabilities Π_{ij}, electron−phonon coupling $\partial\beta/\partial r$, and *localized* force constants (k_i^σ, due to σ bonds)[35]

$$F_{ij} = \delta_{ij}k_i^\sigma + 2\left(\frac{\partial\beta}{\partial r}\right)^2\Pi_{ij} \tag{5}$$

From eq 5, it is clear that diagonal force constants depend on localized quantities (k_i^σ and self-polarizability of the bond Π_{ii}), while off-diagonal interactions depend only on delocalized quantities. To account for this difference, it is fully justified to adopt two different scaling factors for diagonal (x_1) and off-diagonal (x_2) force constants.

The results of the adaptative scaling are shown in Figure 7, where the simulated Raman spectra are plotted. The agreement obtained with experimental data is now excellent, regarding the frequency and dispersion of the α line and the relative intensity and position of the β line. In Figure 7, we also report experimental Raman α lines (dashed vertical lines) of long adamantyl-capped polyynes, recently synthesized in the group of Professor R. R. Tykwinski.[34] Because of the different nature of the end groups, these data have not been included into the fitting procedure. The excellent agreement of the adaptative scaling in predicting also the α frequency of the longest adamantyl-capped polyyne ($N = 10$) shows the soundness of our present approach.

In the Supporting Information, the eigenvectors of the α and β lines obtained from the adaptative linear scaling procedure are also reported. It is important to notice that the shape of the eigenvectors does not significantly change with respect to those reported in Figure 2; this guarantees that all of the physical concepts discussed in section II still hold after scaling.

IV. Conclusions

The role of long-range vibrational interactions in linear carbon chains has been discussed, aiming at the simulation of Raman spectra. The dependence of the frequency of the relevant Raman modes on the effective range of interaction has been rationalized in terms of the results obtained for an infinite chain.[23]

The strong dependence of the Raman-active frequencies upon the DFT functional and, in particular, the effect of the inclusion of exact exchange has been discussed. On this basis, the need

for a suitable scaling procedure for the development of force fields adequate for quantitative predictions of the observed Raman features has been demonstrated, and a new efficient "adaptive linear scaling" has been proposed.

The results presented should be considered to accurately simulate the Raman spectra of a sample of polyynes, which, very recently, have become available thanks to chemical synthesis.[4]

Acknowledgment. The authors gratefully thank Dr. A. Lucotti for helpful scientific discussions and experimental Raman data. The authors express their gratitude to Dr. W. Chalifoux and Professor R. R. Tykwinski of the University of Alberta for sharing with us unique pure samples of adamantyl-capped polyynes of specific chain lengths. This made it possible to extend the adaptative scaling procedure to longer chains than those previously available.[24] This work has been partly supported by grants from the Italian Ministry of Education, University and Research through FIRB projects "Molecular compounds and hybrid nanostructured materials with resonant and non resonant optical properties for photonic devices" (RBNE033KMA) and "Carbon based micro and nano structures" (RBNE019NKS) and by project PRIN "Molecular materials and nanostructures for photonics and nanophotonics" (2004033197).

Appendix A

For the sake of simplicity, we describe the "adapted" x_2 parameter through a linear relationship with a dimensionless parameter (Δf) related to the concept of interaction range

$$x_2 = c\Delta f \tag{A1}$$

$$\Delta f = \frac{|\langle \mathbf{f}_1 \rangle| - |\langle \mathbf{f}_2 \rangle|}{|\langle \mathbf{f}_1 \rangle|} \tag{A2}$$

In eq A2, the vectors $\mathbf{f}_1$ and $\mathbf{f}_2$ represent the first and the second co-diagonals of the force constant matrix **F** restricted to the CC stretching coordinates alone (see Supporting Information). The parameter Δf characterizes the decrease rate of the off-diagonal interactions, and it becomes progressively smaller as the range of interaction increases. For instance, Δf ranges from 0.56 to 0.53 while changing from $N = 4$ to 8 (PBE1PBE/cc-pVTZ force field). The adaptative linear scaling simply assumes x_2 to be a linear function of Δf (eq A2). The coefficient c in eq A1 has to be determined by minimizing the error between simulated Raman spectra and experimental data (the set of Raman data on hydrogen-ended polyynes[24,33] has been considered to determine the best parameters). The adaptative fitting illustrated above has been applied only to the terms belonging to the stretching submatrix. As for the CH stretching force constants, we found just a minor improvement of the figure of merit for the fit (rms of the errors in the vibrational frequencies) by scaling the diagonal CH force constant by 0.883. The interaction force constants between CC and CH stretchings have been kept unscaled in order to avoid extra parameters. The following set of parameters has been obtained for CC stretching force constants: $x_1 = 0.9038$ and $x_2 = 1.6482\ \Delta f$. By using this set of parameters in eq 4, the scaled force field **F′** has been computed, and the Raman spectra reported in Figure 7 have been obtained.

Supporting Information Available: Discussion of the properties of the **F** matrix relative to vibrational long-range interactions and the effect of the DFT functional on the simulated Raman spectra. Nuclear displacements associated with the α and β lines obtained from the adaptative linear scaling scheme of PBE1PBE/cc-pVTZ calculations. Discussion of the relation between phonons of a diatomic linear chain and normal modes of finite chains. This material is available free of charge via the Internet at http://pubs.acs.org.

References and Notes

(1) Cataldo, F. *Carbon* **2004**, *42*, 129.

(2) Lucotti, A.; Tommasini, M.; Del Zoppo, M.; Castiglioni, C.; Zerbi, G.; Cataldo, F.; Casari, C. S.; Li Bassi, A.; Russo, V.; Bogana, M.; Bottani, C. E. *Chem. Phys. Lett.* **2006**, *417*, 78.

(3) Tabata, H.; Fujii, M.; Hayashi, S. *Chem. Phys. Lett.* **2006**, *420*, 166.

(4) Eisler, S.; Slepkov, A. D.; Elliot, E.; Luu, T.; McDonald, R.; Hengmann, F. A.; Tykwinski, R. R. *J. Am. Chem. Soc.* **2005**, *127*, 2666.

(5) (a) Compagnini, G.; Battiato, S.; Puglisi, O.; Baratta, G. A.; Strazzulla, G. *Carbon* **2005**, *43*, 3025. (b) D'Urso, L.; Compagnini, G.; Puglisi, O. *Carbon* **2006**, *44*, 2093.

(6) Ravagnan, L.; Piseri, P.; Bruzzi, M.; Miglio, S.; Bongiorno, G.; Baserga, A.; Casari, C. S.; Li Bassi, A.; Lenardi, C.; Yamaguchi, Y.; Wakabayashi, T.; Bottani, C. E.; Milani, P. *Phys. Rev. Lett.* **2007**, *98*, 216103.

(7) Casari, C. S.; Russo, V.; Li Bassi, A.; Bottani, C. E.; Cataldo, F.; Lucotti, A.; Tommasini, M.; Del Zoppo, M.; Castiglioni, C.; Zerbi, G. *Appl. Phys. Lett.* **2007**, *90*, 013111.

(8) Jones, R. O.; Seifert, G. *Phys. Rev. Lett.* **1997**, *79*, 443.

(9) Saito, M.; Okamoto, Y. *Phys Rev. B* **1999**, *60*, 8939.

(10) Torelli, T.; Mitas, L. *Phys. Rev. Lett.* **2000**, *85*, 1702.

(11) Abdurahman, A.; Shukla, A.; Dolg, M. *Phys. Rev. B* **2002**, *65*, 115106.

(12) Karpfen, A. *J. Phys. C* **1979**, *12*, 3227.

(13) Springborg, M. *J. Phys. C* **1986**, *19*, 4473.

(14) Rusznyak, A.; Zólyomi, V.; Kürti, J.; Yang, S.; Kertesz, M. *Phys. Rev. B* **2005**, *72*, 155420.

(15) Bylaska, E. J.; Weare, J. H.; Kawai, R. *Phys. Rev. B* **1998**, *58*, R7488.

(16) Tongay, S.; Senger, R. T.; Dag, S.; Ciraci, S. *Phys. Rev. Lett.* **2004**, *93*, 136404.

(17) Zhao, X.; Ando, Y.; Liu, Y.; Jinno, M.; Suzuki, T. *Phys. Rev. Lett.* **2003**, *90*, 187401.

(18) Cazzanelli, E.; Castriota, M.; Caputi, L. S.; Cupolillo, A.; Giallombardo, C.; Papagno, L. *Phys. Rev. B* **2007**, *75*, 121405(R).

(19) (a) Nishide, D.; Dohi, H.; Wakabayashi, T.; Nishibori, E.; Aoyagi, S.; Ishida, M.; Kikuchi, S.; Kitaura, R.; Sugai, T.; Sakata, M.; Shinohara, H. *Chem. Phys. Lett.* **2006**, *428*, 356. (b) Nishide, D.; Wakabayashi, T.; Sugai, T.; Kitaura, R.; Kataura, H.; Achiba, Y.; Shinohara, H. *J. Phys. Chem. C* **2007**, *111*, 5178.

(20) Peierls, R. E. *Quantum Theory of Solids*; Oxford University Press: New York, 2001; ISBN 019850781X.

(21) Ashcroft, N. W.; Mermin, N. D. *Solid State Physics*; Saunders: Philadelphia, PA, 1976; ISBN 0030839939.

(22) (a) Gussoni, M.; Castiglioni, C.; Zerbi, G. In *Spectroscopy of Advanced Materials*; Clark, J. H., Hester, R. E., Eds.; Wiley and Sons: New York, 1991. (b) Castiglioni, C.; Tommasini, M.; Zerbi, G. *Philos. Trans. R. Soc. London, Ser. A* **2004**, *362*, 2425. (c) Zerbi, G. In *Vibrational Spectroscopy of Polymers: Principles and Practice*; Everall, N. J., Chalmers, J. M., Griffiths, P. R., Eds.; Wiley: New York, 2007; ISBN 978-0-470-01662-6, and references therein.

(23) Milani, A.; Tommasini, M.; Del Zoppo, M.; Castiglioni, C.; Zerbi, G. *Phys. Rev. B* **2006**, *74*, 153418.

(24) Tabata, H.; Fujii, M.; Hayashi, S.; Doi, T.; Wakabayashi, T. *Carbon* **2006**, *44*, 3168.

(25) Long, D. A. *The Raman Effect: A Unified Treatment of the Theory of Raman Scattering by Molecules*; John Wiley & Sons: New York, 2002.

(26) Wilson, E. B.; Decius, J. C.; Cross, P. C. *Molecular Vibrations: The Theory of Infrared and Raman Vibrational Spectra*; Dover Publications: Mineola, NY, 1980; ISBN 048663941X.

(27) Califano, S. *Vibrational States*; John Wiley & Sons: New York, 1997; ISBN 0471129968.

(28) Frisch, M. J.; Trucks, G. W.; Schlegel, H. B.; Scuseria, G. E.; Robb, M. A.; Cheeseman, J. R.; Montgomery, J. A., Jr.; Vreven, T.; Kudin, K. N.; Burant, J. C.; Millam, J. M.; Iyengar, S. S.; Tomasi, J.; Barone, V.; Mennucci, B.; Cossi, M.; Scalmani, G.; Rega, N.; Petersson, G. A.; Nakatsuji, H.; Hada, M.; Ehara, M.; Toyota, K.; Fukuda, R.; Hasegawa, J.; Ishida, M.; Nakajima, T.; Honda, Y.; Kitao, O.; Nakai, H.; Klene, M.; Li, X.; Knox, J. E.; Hratchian, H. P.; Cross, J. B.; Bakken, V.; Adamo, C.; Jaramillo, J.; Gomperts, R.; Stratmann, R. E.; Yazyev, O.; Austin, A. J.; Cammi, R.; Pomelli, C.; Ochterski, J. W.; Ayala, P. Y.; Morokuma, K.; Voth, G. A.; Salvador, P.; Dannenberg, J. J.; Zakrzewski, V. G.; Dapprich,

S.; Daniels, A. D.; Strain, M. C.; Farkas, O.; Malick, D. K.; Rabuck, A. D.; Raghavachari, K.; Foresman, J. B.; Ortiz, J. V.; Cui, Q.; Baboul, A. G.; Clifford, S.; Cioslowski, J.; Stefanov, B. B.; Liu, G.; Liashenko, A.; Piskorz, P.; Komaromi, I.; Martin, R. L.; Fox, D. J.; Keith, T.; Al-Laham, M. A.; Peng, C. Y.; Nanayakkara, A.; Challacombe, M.; Gill, P. M. W.; Johnson, B.; Chen, W.; Wong, M. W.; Gonzalez, C.; Pople, J. A. *Gaussian 03*, revision C.02; Gaussian, Inc.: Wallingford, CT, 2004.

(29) Yang, S.; Kertesz, M.; Zólyomi, V.; Kürti, J. *J. Phys. Chem. A* **2007**, *111*, 2434.

(30) Zbinden, R. *Infrared Spectroscopy of High Polymers*; Academic Press: New York, 1964.

(31) Scott, A. P.; Radom, L. *J. Phys. Chem.* **1996**, *100*, 16502.

(32) Baker, J.; Jarzecki, A. A.; Pulay, P. *J. Phys. Chem. A* **1998**, *102*, 1412.

(33) Wakabayashi, T.; Tabata, H.; Doi, T.; Nagayama, H.; Okuda, K.; Umeda, R.; Hisaki, I.; Sonoda, M.; Tobe, Y.; Minematsu, T.; Hashimoto, K.; Hayashi, S. *Chem. Phys. Lett.* **2007**, *433*, 296.

(34) (a) Chalifoux, W.; Tykwinski, R. R. Private communication. (b) Lucotti, A.; Tommasini, M.; Fazzi, D.; Del Zoppo, M.; Zerbi, G.; Chalifoux, W.; Tykwinski, R. R. Paper in preparation.

(35) Kakitani, T. *Prog. Theor. Phys.* **1974**, *51*, 656.

(36) Actually, DFT simulations carried out on several hydrogen-capped polyynes (three to five triple bonds) in a slightly bent geometry show equilibrium structures with small deviations $\delta\theta$ of the CCC valence angle from 180° (the maximum value of $\delta\theta$ we have found is 7°). Nevertheless, a comparison between calculated CC stretching frequencies obtained for bent chains and those for the linear ones does not show meaningful differences. The largest frequency shifts are 1 cm^{-1}. This is merely the consequence of a negligible dynamical coupling between bending and stretching vibrations. Moreover, the choice of a linear geometry for oligomers makes it possible to assume the same symmetry for short chains and for the infinite 1D crystal, thus making the comparison easier.

(37) The symbol f_i^n refers to the interactions between equivalent bonds (single or triple) belonging to different cells; f_{ij}^n refers to the interaction between nonequivalent bonds at distance n. The symbols appearing in eq 2 can be collected in a usual matrix representation of the force constant matrix **F** of the infinite chain (see Supporting Information).

(38) The plot of Fig. 3 has been obtained by using force constants transferred from the scaled force field obtained from a PBE1PBE/cc-pVTZ calculation (see discussion in section III), but the same qualitative results are obtained using unscaled DFT force fields of the same molecule.

(39) The choice of the functional PBE1PBE and of the basis set cc-pVTZ is motivated by the fact that it seems to be the method which can better reproduce the relative intensities of the α and β lines (see Figure 1).